

Published in final edited form as:

*Neuroscience*. 2009 February 18; 158(4): 1460–1468. doi:10.1016/j.neuroscience.2008.10.061.

## Interaction of the apolipoprotein E receptors low density lipoprotein receptorrelated protein and sorLA/LR11

Robert Spoelgen<sup>1,4</sup>, Kenneth W. Adams<sup>1,4</sup>, Mirjam Koker<sup>1</sup>, Anne V. Thomas<sup>1</sup>, Olav M. Andersen<sup>2</sup>, Penelope J. Hallett<sup>1</sup>, Kathryn K. Bercury<sup>1</sup>, Daniel F. Joyner<sup>1</sup>, Meihua Deng<sup>1</sup>, William H. Stoothoff<sup>1</sup>, Dudley K. Strickland<sup>3</sup>, Thomas E. Willnow<sup>2</sup>, and Bradley T. Hyman<sup>1,‡</sup>

<sup>1</sup>MassGeneral Institute for Neurodegenerative Disease, Massachusetts General Hospital, Harvard Medical School, Charlestown, MA 02129, USA

<sup>2</sup>Max Delbrück-Center for Molecular Medicine, Berlin, Germany

<sup>3</sup>Center for Vascular and Inflammatory Diseases, University of Maryland School of Medicine, Baltimore, USA

### Abstract

In this study, we examined protein-protein interactions between two neuronal receptors, low density lipoprotein receptor-related protein (LRP) and sorLA/LR11, and found that these receptors interact, as indicated by three independent lines of evidence: co-immunoprecipitation experiments, surface plasmon resonance analysis, and fluorescence lifetime imaging microscopy (FLIM).

Immunocytochemistry experiments revealed widespread co-localization of LRP and sorLA within perinuclear compartments of neurons, while FLIM analysis showed that LRP-sorLA interactions take place within a subset of these compartments.

### Keywords

LRP; sorLA; LR11; LDL receptor

Low density lipoprotein receptor-related protein (LRP) is a large (600 kDa) multifunctional receptor that plays roles in binding and clearance of multiple ligands, including apolipoprotein E (apoE) (Herz and Strickland, 2001), and in trafficking of the Alzheimer's disease-related protein amyloid precursor protein (APP), which impacts amyloid-beta peptide (A $\beta$ ) production in cells (Ulery et al., 2000, Pietrzik et al., 2002, Cam et al., 2005). Furthermore, strong evidence indicates that LRP is involved in signal transduction pathways initiated by N-methyl-D-aspartate receptors as well as platelet-derived growth factor (PDGF) BB (Bacsikai et al., 2000, Loukinova et al., 2002, Boucher et al., 2003). Furin cleavage of LRP within the trans Golgi network during its transit through the secretory pathway leads to formation of a heterodimer consisting of an 85 kDa light chain, containing the transmembrane domain and an intracellular domain with 2 NPXY motifs, and a 515 kDa heavy chain that constitutes the majority of the extracellular domain and contains four distinct cysteine-rich complement-type repeats necessary for ligand binding.

Another member of the low density lipoprotein (LDL) receptor family expressed in neurons that has also been shown to bind apoE in the nervous system is sorLA (Jacobsen et al., 2001,

<sup>‡</sup>To whom correspondence should be addressed: Bradley T. Hyman, M.D., Ph.D., Department of Neurology/ Alzheimer Unit, 114 16th Street, Charlestown, MA 02129, Tel: (617)726-2299, Fax: (617)724-1480, E-mail: E-mail: bhyman@partners.org.

<sup>4</sup>Authors contributed equally.

Taira et al., 2001). SorLA contains a unique combination of modules and may be regarded as a member of a novel family of vacuolar protein sorting 10 protein (Vps10p) receptors, which contain a domain with high homology to the yeast sorting protein Vps10p (Hermans-Borgmeyer et al., 1998). In addition to a Vps10p domain, the luminal domain of sorLA also comprises a cluster of LDL-r class A complement-type repeats and a  $\beta$ -propeller, similar to other LDL receptor family members, as well as six fibronectin type III repeats. Like LRP, sorLA is known to influence APP trafficking and generation of A $\beta$  (Andersen et al., 2005, Offe et al., 2006, Spoelgen et al., 2006) LRP and sorLA are also both known to interact with BACE and modulate its trafficking to and from perinuclear compartments (von Arnim et al., 2005, Spoelgen et al., 2006).

Since these two receptors share ligands, we reasoned that they might form multimeric complexes analogous to those observed with other members of the LDL receptor family, such as VLDL-r/ApoER2 heterodimers (Hiesberger et al., 1999), LRP5/LRP6 interactions implicated in Wnt-signaling (He et al., 2004), and LRP/integrin interactions in the presence of protease/protease inhibitor complexes (Cao et al., 2006). We therefore sought to test the hypothesis that LRP and sorLA interact. Using co-immunoprecipitation experiments and surface plasmon resonance analysis, we demonstrate that LRP and sorLA interact at endogenous levels within neurons as well as when overexpressed within neuroblastoma cells, and that interaction occurs through both their respective luminal domains and cytoplasmic tails. Immunocytochemistry and fluorescence resonance energy transfer (FRET) imaging of endogenous proteins further showed that LRP-sorLA interactions localize to intracellular perinuclear compartments.

## Experimental Procedures

### Cell culture conditions and treatment of cells

Mouse neuroblastoma N2a cells and primary rat cortical neurons were used in this study. N2a cells were maintained in Opti-MEM (Gibco, Gaithersburg, MD) with 5% Fetal Bovine Serum (FBS) at 5% FBS at 37°C, 5% CO<sub>2</sub>. Primary cortical cultures were generated from Sprague Dawley rats at embryonic day 18 as described (Hallett et al., 2006, Spoelgen et al., 2006). After dispersing the neurons in Neurobasal Media (Gibco, Gaithersburg, MD) containing 10% FBS, the cells were plated onto poly-D-lysine- and laminin- (Sigma, St. Louis, MO) coated four-well glass slides (Nalge Nunc International, Naperville, IL). One hour after plating, the media was replaced with Neurobasal media containing 2% B-27 supplement (Gibco, Gaithersburg, MD), within which neurons were maintained for eight days at 37°C, 5% CO<sub>2</sub>.

### Transient transfection and generation of expression constructs

Transient transfections were performed one day after cell plating using FuGENE6 (Roche, Indianapolis, IN) according to the manufacturer's instructions. The following constructs were used in transient transfections: pEGFP-N1 (Clontech), pcDNA3.1-sorLA, -sorLA-flag, -sorLA-GFP, -sorLA $\Delta$ cd, and sorLA-tail were described previously (Andersen et al., 2005, Spoelgen et al., 2006). The sorLA constructs are based on the sequence of accession number: NM\_003105. The constructs encoding the LRP minireceptors (pSec-mLRP1-myc, -myc-mLRP2, -myc-mLRP3, -myc-mLRP4) were previously described (Li et al., 2000, Mikhailenko et al., 2001), as were the pSec-myc-LC & pSec-LC-myc-his constructs (Loukinova et al., 2002).

### Surface plasmon resonance analysis

Interaction between LRP and sorLA was studied by surface plasmon resonance (SPR) analysis on a Biacore 2000 instrument (Biacore, Sweden). Human LRP was purified from placenta as described (Moestrup et al., 1990), and immobilized at pH 3.0 on biacore CM5 chip

corresponding to a receptor density of 19 fmol/mm<sup>2</sup>. A hexa-His-tagged fragment of sorLA including the YWTD-repeated  $\beta$ -propeller and the single EGF-domain followed by the 11 CR-domains (residues 728-1526) was expressed and secreted from EBNA293 cells and purified using Ni<sup>2+</sup>-ion affinity chromatography as previously reported (Andersen et al., 2005). Samples were analyzed in 10 mM HEPES, pH 7.4, 150 mM NaCl, 1.5 mM CaCl<sub>2</sub>, 1.0 mM EGTA and 0.005% tween-20 at a flow of 5  $\mu$ l/min. Sample and running buffer were identical. Regeneration of the sensor chip after each analysis cycle was performed with alternating pulses of 1.6 M glycine-HCl buffer, pH 3.0 and 0.01% SDS. The instrument response is expressed in relative response units (RU), i.e. the difference in response between protein and control flow channel. Kinetic parameters were determined using the BIAevaluation 3.1 software using a Langmuir 1:1 binding model and simultaneous fitting of all curves in the concentration range from 50-2000 nM (global fitting).

### Co-immunoprecipitation experiments

For co-immunoprecipitation of endogenous LRP and sorLA, mouse brain extracts were prepared in 1% Triton X-100 lysis buffer (50 mM Tris-HCl, pH 8.0, 150 mM NaCl, 1% Triton X-100, supplemented with Complete Protease Inhibitor cocktail [Roche, Branchburg, NJ]). Extracts were pre-cleared with Protein G Sepharose beads (Sigma-Aldrich, St. Louis, MO) for 1 h at 4°C, and then incubated with either non-immunune mouse IgG or mouse anti-LRP 11H4 antibody overnight at 4°C. Protein G Sepharose beads were added and samples incubated for 1 h at 4°C. Beads were washed three times with 1% CHAPSO buffer (50 mM HEPES, pH 7.4, 150 mM NaCl, 2 mM EDTA, 1% CHAPSO, supplemented with Complete Protease Inhibitor cocktail) and boiled in 2x Tris-Glycine SDS sample buffer. Western blots were performed as described below.

Co-immunoprecipitations of overexpressed proteins were performed on N2a cells co-transfected with the indicated constructs. Twenty-four to forty-eight h after transfection, cells were harvested and lysed in 1% Triton X-100 buffer. Lysates were incubated with  $\mu$ MACS magnetic beads conjugated either to mouse anti-GFP, mouse anti-myc, or mouse anti-his antibody (Miltenyi Biotec, Auburn, CA) for 2-3 h at 4°C, and then purified using  $\mu$ MACS magnetic separation columns (Miltenyi Biotec, Auburn, CA) according to the manufacturer's instructions.

### Western blotting

Lysate and immunoprecipitation fractions were boiled for 5 min in Tris-Glycine SDS sample buffer (Invitrogen, Gaithersburg, MD) and electrophoresed through Tris-glycine polyacrylamide gels (Novex, San Diego, CA), followed by transfer of the protein to PVDF membrane (Millipore, Bedford, MA). Membranes were incubated in blocking buffer (5% nonfat dried milk in Tris-buffered saline (TBS), pH 7.4 containing 0.05% Tween-20) for 1 h prior to incubation with primary antibody diluted in fresh blocking buffer for 1 h at room temperature. The following primary antibodies were used: mouse anti-sorLA (BD Biosciences, San Jose, CA), rabbit anti-N-terminal sorLA, rabbit anti-Cterminal sorLA, goat anti-sorLA (all provided by Anders Nykjaer, University of Aarhus, Denmark), mouse anti-LRP/LC 11H4 (Kowal et al., 1989), mouse anti-85 kDa LRP 5A6 (Strickland et al., 1990) (both provided by Dr. D. Strickland), mouse anti-c-myc 9E10 (Abcam, Cambridge, MA), and mouse anti-GFP (Abcam). Membranes were washed with TBS containing 0.05% Tween-20 (TBST), and incubated with HRP-conjugated secondary antibody diluted in fresh blocking buffer for 1 hour at room temperature. Membranes were washed with TBST, and proteins were detected via chemiluminescence (ECL Western Blotting Detection reagent, Amersham Biosciences, Piscataway, NJ).

## Immunocytochemistry

After fixation in 4% paraformaldehyde for 10 minutes, cells were washed twice in TBS and permeabilized in 0.5% Triton X-100 for 10 minutes. Cells were then blocked in 1.5% normal donkey serum (NDS), followed by incubation with primary antibodies diluted in 1.5% NDS overnight at 4°C. The following primary antibodies were used for immunocytochemistry: mouse anti-LRP 5A6, rabbit anti-N-terminal sorLA, goat anti-sorLA. After three washes in TBS, secondary antibodies conjugated to Alexa Fluor 488 (Invitrogen, Gaithersburg, MD), Cy3, or Cy5 (Jackson ImmunoResearch, West Grove, PA) were applied, diluted in 1.5% NDS, and incubated for 1 h at room temperature followed by three washes in TBS. Slides were coverslipped using GVA mounting solution (Zymed, South San Francisco, CA) and examined by confocal microscopy.

## Detection of fluorescence resonance energy transfer (FRET) using fluorescence lifetime imaging microscopy (FLIM)

FLIM allows for the assessment of FRET between two fluorophores labeling different epitopes within intact cells. If these fluorophores are in close proximity (<10nm) of each other, some of the donor fluorophore's emission energy is non-radiatively transferred to the acceptor fluorophore. This results in a decrease in donor fluorescence lifetime, which is inversely related to the distance between the fluorophores and can be measured by FLIM.

We employed a validated FLIM technique based on multiphoton microscopy (Bacskaï et al., 2003) to compare the proximity of endogenous LRP and endogenous sorLA in rat primary neurons. Lifetime imaging was performed on a multiphoton microscope (Radiance 2000, Bio-Rad, Hercules, CA) using a femtosecond mode-locked Ti:Sapphire Laser (Mai Tai; Spectra-Physics, Mountain View, CA) at 800 nm. Data were collected with a high-speed photomultiplier tube (MCP R3809; Hamamatsu, Hamamatsu City, Japan) and a time correlated single-photon counting (TCSPC) acquisition board (SPC 830; Becker&Hickl, Berlin, Germany). Donor fluorophore lifetimes were determined by fitting the data to exponential decay curves using SPC Image (Becker&Hickl, Berlin, Germany).

## Statistical Analysis

Statistical analysis was performed using a two-sample t-test in StatView for Windows, Version 5.0.1 (SAS Institute, Inc). Differences between samples were considered significant if  $p < 0.05$ .

## Results

### LRP and sorLA co-immunoprecipitate from mouse brain lysates and N2a neuroblastoma cells

Since LRP and sorLA are both highly expressed in the nervous system, interaction between these receptors was examined by immunoprecipitation of LRP from mouse brain lysates followed by Western blot for sorLA. Co-immunoprecipitation of sorLA with 11H4 anti-LRP antibody, but not with nonimmune mouse IgG, indicated that these receptors interact at endogenous levels (Fig. 1A). To determine whether LRP and sorLA would co-immunoprecipitate from a neuronal cell line, Neuro2a (N2a) cells were transfected with either a plasmid encoding sorLA fused to a carboxy-terminal GFP tag (sorLA-GFP) or with a plasmid encoding GFP alone, followed by immunoprecipitation with anti-GFP antibody and Western blot for endogenous LRP. As shown in figure 1B, expression of sorLA-GFP resulted in co-immunoprecipitation of LRP (lanes 3-4), while expression of GFP alone did not (lanes 1-2). Of note, both endogenous and exogenous LRP light chain consistently ran at a higher molecular weight in N2a cells compared to mouse brain lysates. Differential glycosylation of LRP light

chain has been reported (May et al., 2003), which likely accounts for the differences in molecular weight observed here.

### LRP-sorLA interactions occur through the LRP light chain

LRP and sorLA bind several common ligands, including apoE, PDGF-BB, and uPA/PAI-1 complexes, suggesting that LRP-sorLA interactions may result from their acting as co-receptors for a common ligand. Whereas sorLA contains a single LDLR-type ligand-binding domain (LBD), LRP contains four such domains, which exhibit unique, though overlapping, ligand-binding specificities. Thus, if LRP and sorLA do act as co-receptors for a common ligand, their interaction may be dependent on a particular LBD(s) of LRP. To test this possibility, N2a cells were co-transfected with plasmids encoding sorLA-GFP and each of four mini-LRP receptors, in which the LRP extracellular domain was truncated to encode only one of its four LBDs (mLRP1-myc, myc-mLRP2, myc-mLRP3, and myc-mLRP4). SorLA-GFP was then immunoprecipitated with anti-GFP antibody and co-immunoprecipitation of each mLRP receptor was examined by Western blot with anti-myc antibody. As shown in figure 2A, all four mLRP receptors co-immunoprecipitated with sorLA-GFP (lanes 2-5), while mLRP2 did not in the absence of co-transfection with sorLA-GFP (lane 1). The interaction between sorLA and all four mLRP receptors was further confirmed by complementary immunoprecipitation of the myc-tagged mLRP receptors using anti-myc antibody followed by Western blot for sorLA (data not shown). Of note, both the furin-cleaved (lower bands) and -uncleaved (upper bands) mLRP receptors co-immunoprecipitated with sorLA-GFP, indicating that sorLA can interact with both immature and mature forms of LRP.

As an additional control experiment to ensure that co-immunoprecipitation was not due to nonspecific aggregation of the receptors upon membrane solubilization, separate cultures of N2a cells were transfected with either a plasmid encoding mLRP2 or a plasmid encoding sorLA-GFP. Immediately after suspending the cells in 1% Triton X-100 lysis buffer, the samples were combined and immunoprecipitation with anti-GFP antibody was conducted as above. The absence of co-immunoprecipitation of mLRP2 with sorLA-GFP when transfected separately (Fig. 2B, lanes 5 and 6) indicates that co-immunoprecipitation was not an artifact of membrane solubilization and was dependent on their co-expression within the same culture.

The co-immunoprecipitation of all four mLRP receptors with sorLA suggests that LRP-sorLA interactions either occur through each of the four LRP LBDs or, alternatively, occur independently of the LRP LBDs. To distinguish between these possibilities, the co-immunoprecipitation of LRP light chain (LC), which lacks LBDs, with sorLA-GFP was tested as described above following co-transfection into N2a cells. As shown in figure 2C, LC co-immunoprecipitated from cells expressing sorLA-GFP, but not from cells expressing GFP, indicating that LRP-sorLA interactions can occur through the LRP light chain, independent of the LRP LBDs.

### LRP light chain and sorLA exhibit luminal and cytoplasmic domain interactions

The LRP light chain comprises the LRP transmembrane domain with a 476-amino acid luminal/extracellular domain (N-terminal) and a 100-amino acid cytoplasmic tail (C-terminal) (Herz et al., 1990). To examine potential interaction between the luminal portions of LRP light chain and sorLA, co-immunoprecipitation of a truncated form of sorLA lacking its cytoplasmic tail (sorLA $\Delta$ cd) with LRP light chain was tested. N2a cells were transfected with sorLA $\Delta$ cd both with and without LRP light chain containing a C-terminal histidine tag (LC-his), followed by immunoprecipitation with anti-his tag antibody. Expression of LC-his resulted in the co-immunoprecipitation of sorLA $\Delta$ cd, whereas sorLA $\Delta$ cd was not immunoprecipitated in the absence of LC-his (Fig. 3A, lanes 4 and 5), demonstrating that LRP light chain and sorLA can interact via their respective luminal domains.



As an additional measure to confirm the LRP-sorLA luminal domain interaction, surface plasmon resonance analysis was utilized. Purified LRP was immobilized on a Biacore sensor chip to which binding of the sorLA luminal domain was examined. Representative sensorgrams for the binding of 0.05, 0.10, 0.20, 0.50, 1.0, and 2.0  $\mu\text{M}$  of the sorLA luminal domain to LRP are shown, where increases in the response levels correspond to higher sorLA luminal domain concentrations (Fig. 3B). Fitting of the binding curves estimates a dissociation constant  $K_D \sim 36.5$  nM (rate constants:  $k_{\text{on}} \sim 4.11 \times 10^3$  (1/Ms);  $k_{\text{off}} \sim 1.5 \times 10^{-4}$  (1/s)). Taken together, both co-immunoprecipitation studies and surface plasmon resonance analysis demonstrate that the luminal/extracellular domains of LRP and sorLA are sufficient to mediate the interaction of the receptors.

To lastly examine whether the cytoplasmic tails of LRP and sorLA also interact, a sorLA-tail construct was employed, which encodes a truncated form of sorLA lacking its entire luminal/extracellular domain, and tested whether it would co-immunoprecipitate with myc-mLRP2 from co-transfected N2a cells. Co-immunoprecipitation of the sorLA-tail with mLRP2 demonstrated that, independent of the luminal domain interactions, the C-terminal cytoplasmic domains of LRP and sorLA can interact (Fig. 3C). Control experiments on cells expressing only sorLA-tail or only mLRP2 showed no non-specific co-immunoprecipitation.

Collectively, the data shown above suggest that both the luminal/extracellular and cytoplasmic domains of sorLA and LRP can interact. This is in line with previous studies that have demonstrated that LRP can interact with other transmembrane proteins, such as amyloid precursor protein, via both its extracellular and cytoplasmic domains (Kinoshita et al., 2001).

### LRP-sorLA interactions in primary neurons localize to perinuclear compartments

LRP functions largely at the cell surface where it mediates the internalization of numerous ligands, whereas sorLA functions primarily among intracellular compartments where it influences trafficking of proteins including APP. To examine where within neurons LRP and sorLA co-localize, rat primary neurons were subjected to immunocytochemistry. Neurons were immunostained for LRP with mouse 5A6 antibody, visualized by Alexa488, and for sorLA with a goat anti-sorLA antibody, visualized by Cy3. Inspection of the staining pattern revealed extensive co-localization of LRP and sorLA within perinuclear vesicular compartments (Fig. 4A), suggesting that LRP-sorLA interactions may occur in such compartments. More distal vesicles contained only LRP, which highlights the relevance of LRP for uptake processes.

To determine whether LRP-sorLA interactions localize to perinuclear compartments, fluorescence lifetime imaging microscopy (FLIM) was employed, a fluorescence resonance energy transfer (FRET)-based technique in which the lifetime of a donor fluorophore (Alexa488) is measured in the presence and absence of an acceptor fluorophore (Cy3). Proximity of  $< 10$  nm between donor and acceptor fluorophores enables FRET, resulting in a shortened lifetime of the donor fluorophore. Additionally, FLIM reveals the subcellular localization of FRETing populations of fluorophores by measuring the donor fluorophore lifetime in a pixel-by-pixel manner. We developed a FLIM assay in which rat primary neurons were immunostained for endogenous LRP with mouse anti-N-terminal 5A6 antibody, which was labeled with the donor fluorophore Alexa488. In the absence of the acceptor fluorophore Cy3, the donor fluorophore exhibited an average lifetime of  $2253 \pm 13$  ps. When endogenous sorLA was co-immunostained with rabbit anti-N-terminal sorLA antibody and acceptor fluorophore Cy3, the average lifetime of the donor fluorophore was shortened to  $2093 \pm 71$  ps (Fig. 4B), further demonstrating interaction between LRP and sorLA. Figure 4C shows representative images of the FLIM data in which lifetime values are depicted as pseudocolored pixels, with orange pixels indicating close proximity between the receptors. Examination of these images showed that, consistent with the immunocytochemistry analysis, LRP-sorLA

interactions localize to perinuclear compartments, and further show the relevance of their interaction within intact neurons.

## Discussion

Given multiple parallels in the biology of LRP and sorLA, including structural similarities and shared ligands (e.g. apoE and APP), we tested the hypothesis that LRP and sorLA interact. Several independent lines of evidence suggest that this is the case. First of all, endogenous LRP and sorLA co-immunoprecipitate from brain homogenates. Co-immunoprecipitation experiments with modified forms of LRP and sorLA identified two sites of interaction: one between the luminal/extracellular domains of sorLA and the LRP light chain, and one between the respective C-terminal cytoplasmic tails. Previous studies have shown that the C-terminus of LRP interacts with APP indirectly via the cytosolic adaptor protein Fe65 (Kinoshita et al., 2001), suggesting that an adaptor protein may also mediate the LRP-sorLA C-terminal interaction. The luminal/extracellular domains appear to interact directly, as shown here by both co-immunoprecipitation and surface plasmon resonance studies, which demonstrate that the luminal domain of sorLA can interact with LRP directly and with high affinity ( $K_D \sim 36$  nM).

We also evaluated where within the cell the LRP-sorLA interaction takes place. We reasoned that if it were important for ligand binding, it would be prominent at the cell surface. However, immunocytochemistry experiments on primary neurons instead revealed overlap primarily within perinuclear vesicles characteristic of secretory and/or recycling compartments. Fluorescence resonance energy transfer experiments confirmed close proximity between LRP and sorLA, indicative of protein-protein interaction, largely within perinuclear compartments of primary neurons.

Taken together, our data indicate that LRP and sorLA interact via both their luminal/extracellular and cytoplasmic domains, and that LRP-sorLA interactions occur in neurons specifically within perinuclear compartments likely of the secretory and/or recycling pathways. The role of these interactions remains unclear. Localization of LRP-sorLA interactions to perinuclear compartments, compartments in which sorLA affects trafficking of APP, suggests that sorLA may likewise influence trafficking of LRP within secretory or recycling pathways. However, whereas overexpression of sorLA results in reduced levels of APP at the cell surface due to its retention in perinuclear compartments (Andersen et al., 2005), no such effect of sorLA on surface levels of LRP was observed (data not shown).

The observation that LRP and sorLA interact may prove of interest in studies related to Alzheimer's disease. The APOE gene, which encodes a common ligand of both sorLA and LRP, is the strongest known genetic risk factor for late onset Alzheimer's disease (Roses, 1996). APP, whose degradation into A $\beta$  is thought to be a primary pathogenic event in Alzheimer's disease, is also known to interact with multiple members of the LDL receptor family, including LRP and sorLA, as well as apoER2 and LRP1B (Trommsdorff et al., 1998, Kinoshita et al., 2001, Cam et al., 2004, Andersen et al., 2005, Andersen et al., 2006, Fuentealba et al., 2007). Both LRP and sorLA facilitate APP trafficking and modulate A $\beta$  generation (Ulery et al., 2000, Pietrzik et al., 2002, Andersen et al., 2005, Cam et al., 2005, Spoelgen et al., 2006). Moreover, the SORL1 gene itself has been recently implicated as a site of genetic risk for Alzheimer's disease, and sorLA expression is reduced in the brain of Alzheimer's disease patients (Scherzer et al., 2004, Rogaeva et al., 2007). Intriguingly, sorLA appears to act as a mediator of retention of APP in the trans-Golgi as part of the retromer complex, likely in association with GGA and PACS-1 (Spoelgen et al., 2006, Nielsen et al., 2007, Schmidt et al., 2007), whereas LRP appears to mediate trafficking of APP to lipid rafts (Ulery et al., 2000, Cam et al., 2005, Yoon et al., 2007). The molecular consequence of the LRP-sorLA

interactions on APP trafficking remains to be addressed. Given the role of sorLA as a sorting receptor that shuttles proteins to the trans Golgi network, we postulate that sorLA could regulate release of APP towards the cell surface, chaperoned by LRP.

## Acknowledgments

We thank Dr. Anthonie W. Dunah and Dr. Uwe Beffert for reagents and assistance, and Lauren Herl for technical assistance. Supported by NIH AG 12406, NIH AG 15379, a research fellowship of the Deutsche Forschungsgemeinschaft to AVT (TH1129/1-1), a grant from the American Health Assistance Foundation (A2005-202) and grants HL50784 & HL54710 to DKS.

## Abbreviations

A $\beta$ , amyloid- $\beta$   
 apoE, apolipoprotein E  
 apoER2, apolipoprotein E receptor-2  
 APP, amyloid precursor protein  
 FLIM, fluorescence lifetime imaging microscopy  
 FRET, fluorescence resonance energy transfer  
 GFP, green fluorescent protein  
 GGA, golgi associated, gamma adaptin ear containing, ARF binding protein  
 LBD, ligand-binding domain  
 LC, LRP light chain  
 LDL-r, low density lipoprotein receptor  
 LRP, low density lipoprotein receptor-related protein  
 mLRP, mini-LRP receptor  
 PACS-1, phosphofurin acidic cluster sorting protein 1  
 PDGF, platelet-derived growth factor  
 VLDL-r, very low density lipoprotein receptor  
 Vsp10p, vacuolar protein sorting 10 protein

## References

- Andersen OM, Reiche J, Schmidt V, Gotthardt M, Spoelgen R, Behlke J, von Arnim CA, Breiderhoff T, Jansen P, Wu X, Bales KR, Cappai R, Masters CL, Gliemann J, Mufson EJ, Hyman BT, Paul SM, Nykjaer A, Willnow TE. Neuronal sorting protein-related receptor sorLA/LR11 regulates processing of the amyloid precursor protein. *Proc Natl Acad Sci U S A* 2005;102:13461–13466. [PubMed: 16174740]
- Andersen OM, Schmidt V, Spoelgen R, Gliemann J, Behlke J, Galatis D, McKinstry WJ, Parker MW, Masters CL, Hyman BT, Cappai R, Willnow TE. Molecular dissection of the interaction between amyloid precursor protein and its neuronal trafficking receptor SorLA/LR11. *Biochemistry* 2006;45:2618–2628. [PubMed: 16489755]
- Bacskai BJ, Skoch J, Hickey GA, Allen R, Hyman BT. Fluorescence resonance energy transfer determinations using multiphoton fluorescence lifetime imaging microscopy to characterize amyloid-beta plaques. *J Biomed Opt* 2003;8:368–375. [PubMed: 12880341]
- Bacskai BJ, Xia MQ, Strickland DK, Rebeck GW, Hyman BT. The endocytic receptor protein LRP also mediates neuronal calcium signaling via N-methyl-D-aspartate receptors. *Proc Natl Acad Sci U S A* 2000;97:11551–11556. [PubMed: 11016955]
- Boucher P, Gotthardt M, Li WP, Anderson RG, Herz J. LRP: role in vascular wall integrity and protection from atherosclerosis. *Science* 2003;300:329–332. [PubMed: 12690199]
- Cam JA, Zerbinatti CV, Knisely JM, Hecimovic S, Li Y, Bu G. The low density lipoprotein receptor-related protein 1B retains beta-amyloid precursor protein at the cell surface and reduces amyloid-beta peptide production. *J Biol Chem* 2004;279:29639–29646. [PubMed: 15126508]



- Cam JA, Zerbinatti CV, Li Y, Bu G. Rapid endocytosis of the low density lipoprotein receptor-related protein modulates cell surface distribution and processing of the beta-amyloid precursor protein. *J Biol Chem* 2005;280:15464–15470. [PubMed: 15705569]
- Cao C, Lawrence DA, Li Y, Von Arnim CA, Herz J, Su EJ, Makarova A, Hyman BT, Strickland DK, Zhang L. Endocytic receptor LRP together with tPA and PAI-1 coordinates Mac-1-dependent macrophage migration. *Embo J* 2006;25:1860–1870. [PubMed: 16601674]
- Fuentealba RA, Barria MI, Lee J, Cam J, Araya C, Escudero CA, Inestrosa NC, Bronfman FC, Bu G, Marzolo MP. ApoER2 expression increases Abeta production while decreasing Amyloid Precursor Protein (APP) endocytosis: Possible role in the partitioning of APP into lipid rafts and in the regulation of gamma-secretase activity. *Mol Neurodegener* 2007;2:14. [PubMed: 17620134]
- Hallett PJ, Spoelgen R, Hyman BT, Standaert DG, Dunah AW. Dopamine D1 activation potentiates striatal NMDA receptors by tyrosine phosphorylation-dependent subunit trafficking. *J Neurosci* 2006;26:4690–4700. [PubMed: 16641250]
- He X, Semenov M, Tamai K, Zeng X. LDL receptor-related proteins 5 and 6 in Wnt/beta-catenin signaling: arrows point the way. *Development* 2004;131:1663–1677. [PubMed: 15084453]
- Hermans-Borgmeyer I, Hampe W, Schinke B, Methner A, Nykjaer A, Susens U, Fenger U, Herbarth B, Schaller HC. Unique expression pattern of a novel mosaic receptor in the developing cerebral cortex. *Mech Dev* 1998;70:65–76. [PubMed: 9510025]
- Herz J, Kowal RC, Goldstein JL, Brown MS. Proteolytic processing of the 600 kd low density lipoprotein receptor-related protein (LRP) occurs in a trans-Golgi compartment. *Embo J* 1990;9:1769–1776. [PubMed: 2112085]
- Herz J, Strickland DK. LRP: a multifunctional scavenger and signaling receptor. *J Clin Invest* 2001;108:779–784. [PubMed: 11560943]
- Hiesberger T, Trommsdorff M, Howell BW, Goffinet A, Mumby MC, Cooper JA, Herz J. Direct binding of Reelin to VLDL receptor and ApoE receptor 2 induces tyrosine phosphorylation of disabled-1 and modulates tau phosphorylation. *Neuron* 1999;24:481–489. [PubMed: 10571241]
- Jacobsen L, Madsen P, Jacobsen C, Nielsen MS, Gliemann J, Petersen CM. Activation and functional characterization of the mosaic receptor SorLA/LR11. *J Biol Chem* 2001;276:22788–22796. [PubMed: 11294867]
- Kinoshita A, Whelan CM, Smith CJ, Mikhailenko I, Rebeck GW, Strickland DK, Hyman BT. Demonstration by fluorescence resonance energy transfer of two sites of interaction between the low-density lipoprotein receptor-related protein and the amyloid precursor protein: role of the intracellular adapter protein Fe65. *J Neurosci* 2001;21:8354–8361. [PubMed: 11606623]
- Kowal RC, Herz J, Goldstein JL, Esser V, Brown MS. Low density lipoprotein receptor-related protein mediates uptake of cholesteryl esters derived from apoprotein E-enriched lipoproteins. *Proc Natl Acad Sci U S A* 1989;86:5810–5814. [PubMed: 2762297]
- Li Y, Marzolo MP, van Kerkhof P, Strous GJ, Bu G. The YXXL motif, but not the two NPXY motifs, serves as the dominant endocytosis signal for low density lipoprotein receptor-related protein. *J Biol Chem* 2000;275:17187–17194. [PubMed: 10747918]
- Loukinova E, Ranganathan S, Kuznetsov S, Gorlatova N, Migliorini MM, Loukinov D, Ulery PG, Mikhailenko I, Lawrence DA, Strickland DK. Platelet-derived growth factor (PDGF)-induced tyrosine phosphorylation of the low density lipoprotein receptor-related protein (LRP). Evidence for integrated co-receptor function between LRP and the PDGF. *J Biol Chem* 2002;277:15499–15506. [PubMed: 11854294]
- May P, Bock HH, Nimpf J, Herz J. Differential glycosylation regulates processing of lipoprotein receptors by gamma-secretase. *J Biol Chem* 2003;278:37386–37392. [PubMed: 12871934]
- Mikhailenko I, Battey FD, Migliorini M, Ruiz JF, Argraves K, Moayeri M, Strickland DK. Recognition of alpha 2-macroglobulin by the low density lipoprotein receptor-related protein requires the cooperation of two ligand binding cluster regions. *J Biol Chem* 2001;276:39484–39491. [PubMed: 11507091]
- Moestrup SK, Kaltoft K, Sottrup-Jensen L, Gliemann J. The human alpha 2-macroglobulin receptor contains high affinity calcium binding sites important for receptor conformation and ligand recognition. *J Biol Chem* 1990;265:12623–12628. [PubMed: 1695632]

- Nielsen MS, Gustafsen C, Madsen P, Nyengaard JR, Hermey G, Bakke O, Mari M, Schu P, Pohlmann R, Dennes A, Petersen CM. Sorting by the cytoplasmic domain of the amyloid precursor protein binding receptor SorLA. *Mol Cell Biol* 2007;27:6842–6851. [PubMed: 17646382]
- Offe K, Dodson SE, Shoemaker JT, Fritz JJ, Gearing M, Levey AI, Lah JJ. The lipoprotein receptor LR11 regulates amyloid beta production and amyloid precursor protein traffic in endosomal compartments. *J Neurosci* 2006;26:1596–1603. [PubMed: 16452683]
- Pietrzik CU, Busse T, Merriam DE, Weggen S, Koo EH. The cytoplasmic domain of the LDL receptor-related protein regulates multiple steps in APP processing. *Embo J* 2002;21:5691–5700. [PubMed: 12411487]
- Rogaeva E, Meng Y, Lee JH, Gu Y, Kawarai T, Zou F, Katayama T, Baldwin CT, Cheng R, Hasegawa H, Chen F, Shibata N, Lunetta KL, Pardossi-Piquard R, Bohm C, Wakutani Y, Cupples LA, Cuenco KT, Green RC, Pinessi L, Rainero I, Sorbi S, Bruni A, Duara R, Friedland RP, Inzelberg R, Hampe W, Bujo H, Song YQ, Andersen OM, Willnow TE, Graff-Radford N, Petersen RC, Dickson D, Der SD, Fraser PE, Schmitt-Ulms G, Younkin S, Mayeux R, Farrer LA, St George-Hyslop P. The neuronal sortilin-related receptor SORL1 is genetically associated with Alzheimer disease. *Nat Genet* 2007;39:168–177. [PubMed: 17220890]
- Roses AD. Apolipoprotein E alleles as risk factors in Alzheimer's disease. *Annu Rev Med* 1996;47:387–400. [PubMed: 8712790]
- Scherzer CR, Offe K, Gearing M, Rees HD, Fang G, Heilman CJ, Schaller C, Bujo H, Levey AI, Lah JJ. Loss of apolipoprotein E receptor LR11 in Alzheimer disease. *Arch Neurol* 2004;61:1200–1205. [PubMed: 15313836]
- Schmidt V, Sporbert A, Rohe M, Reimer T, Rehm A, Andersen OM, Willnow TE. SorLA/LR11 regulates processing of amyloid precursor protein via interaction with adaptors GGA and PACS-1. *J Biol Chem* 2007;282:32956–32964. [PubMed: 17855360]
- Spoelgen R, von Arnim CA, Thomas AV, Peltan ID, Koker M, Deng A, Irizarry MC, Andersen OM, Willnow TE, Hyman BT. Interaction of the cytosolic domains of sorLA/LR11 with the amyloid precursor protein (APP) and beta-secretase beta-site APP-cleaving enzyme. *J Neurosci* 2006;26:418–428. [PubMed: 16407538]
- Strickland DK, Ashcom JD, Williams S, Burgess WH, Migliorini M, Argraves WS. Sequence identity between the alpha 2-macroglobulin receptor and low density lipoprotein receptor-related protein suggests that this molecule is a multifunctional receptor. *J Biol Chem* 1990;265:17401–17404. [PubMed: 1698775]
- Taira K, Bujo H, Hirayama S, Yamazaki H, Kanaki T, Takahashi K, Ishii I, Miida T, Schneider WJ, Saito Y. LR11, a mosaic LDL receptor family member, mediates the uptake of ApoE-rich lipoproteins in vitro. *Arterioscler Thromb Vasc Biol* 2001;21:1501–1506. [PubMed: 11557679]
- Trommsdorff M, Borg JP, Margolis B, Herz J. Interaction of cytosolic adaptor proteins with neuronal apolipoprotein E receptors and the amyloid precursor protein. *J Biol Chem* 1998;273:33556–33560. [PubMed: 9837937]
- Ulery PG, Beers J, Mikhaillenko I, Tanzi RE, Rebeck GW, Hyman BT, Strickland DK. Modulation of beta-amyloid precursor protein processing by the low density lipoprotein receptor-related protein (LRP). Evidence that LRP contributes to the pathogenesis of Alzheimer's disease. *J Biol Chem* 2000;275:7410–7415. [PubMed: 10702315]
- von Arnim CA, Kinoshita A, Peltan ID, Tangredi MM, Herl L, Lee BM, Spoelgen R, Hshieh TT, Ranganathan S, Battey FD, Liu CX, Bacskai BJ, Sever S, Irizarry MC, Strickland DK, Hyman BT. The low density lipoprotein receptor-related protein (LRP) is a novel beta-secretase (BACE1) substrate. *J Biol Chem* 2005;280:17777–17785. [PubMed: 15749709]
- Yoon IS, Chen E, Busse T, Repetto E, Lakshmana MK, Koo EH, Kang DE. Low-density lipoprotein receptor-related protein promotes amyloid precursor protein trafficking to lipid rafts in the endocytic pathway. *Faseb J* 2007;21:2742–2752. [PubMed: 17463224]

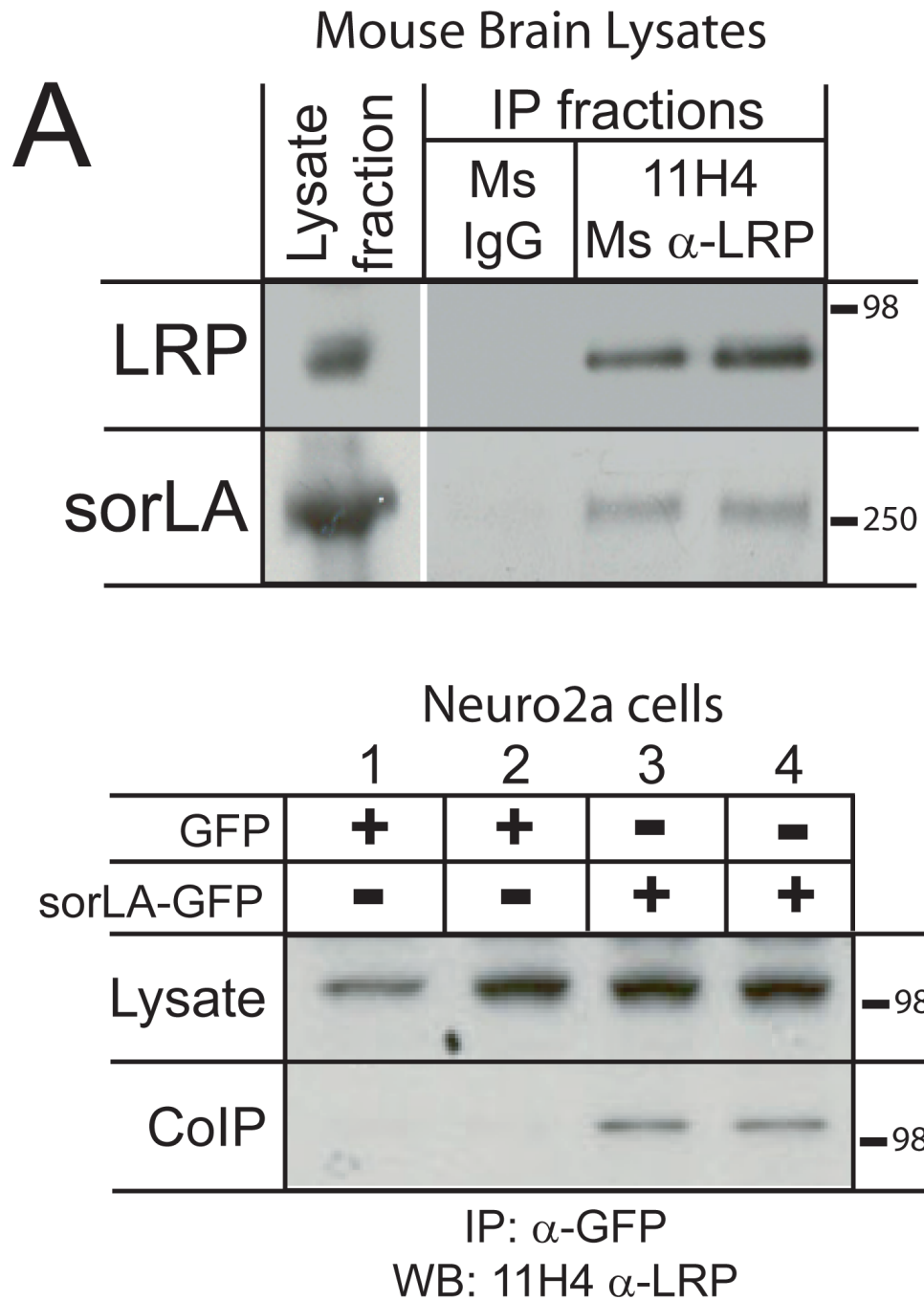


**Figure 1. LRP and sorLA co-immunoprecipitate from mouse brain lysates and Neuro2a cells**  
**A:** Mouse brain extracts were subjected to immunoprecipitation with either non-immune mouse IgG (lane 2) or mouse anti-LRP 11H4 antibody (lanes 3 and 4). Lysate and immunoprecipitation fractions were then subjected to SDS-PAGE and Western blot with anti-LRP 11H4 and anti-sorLA antibodies (n = 4).  
**B:** N2a cells were transfected with either pEGFP-N1 or pcDNA3.1-sorLA-GFP. Forty-eight h after transfection, cell lysates were harvested and subjected to immunoprecipitation with anti-GFP antibody coupled to magnetic beads. Lysate and immunoprecipitation fractions were then subjected to SDS-PAGE and Western blot for endogenous LRP (n = 4).

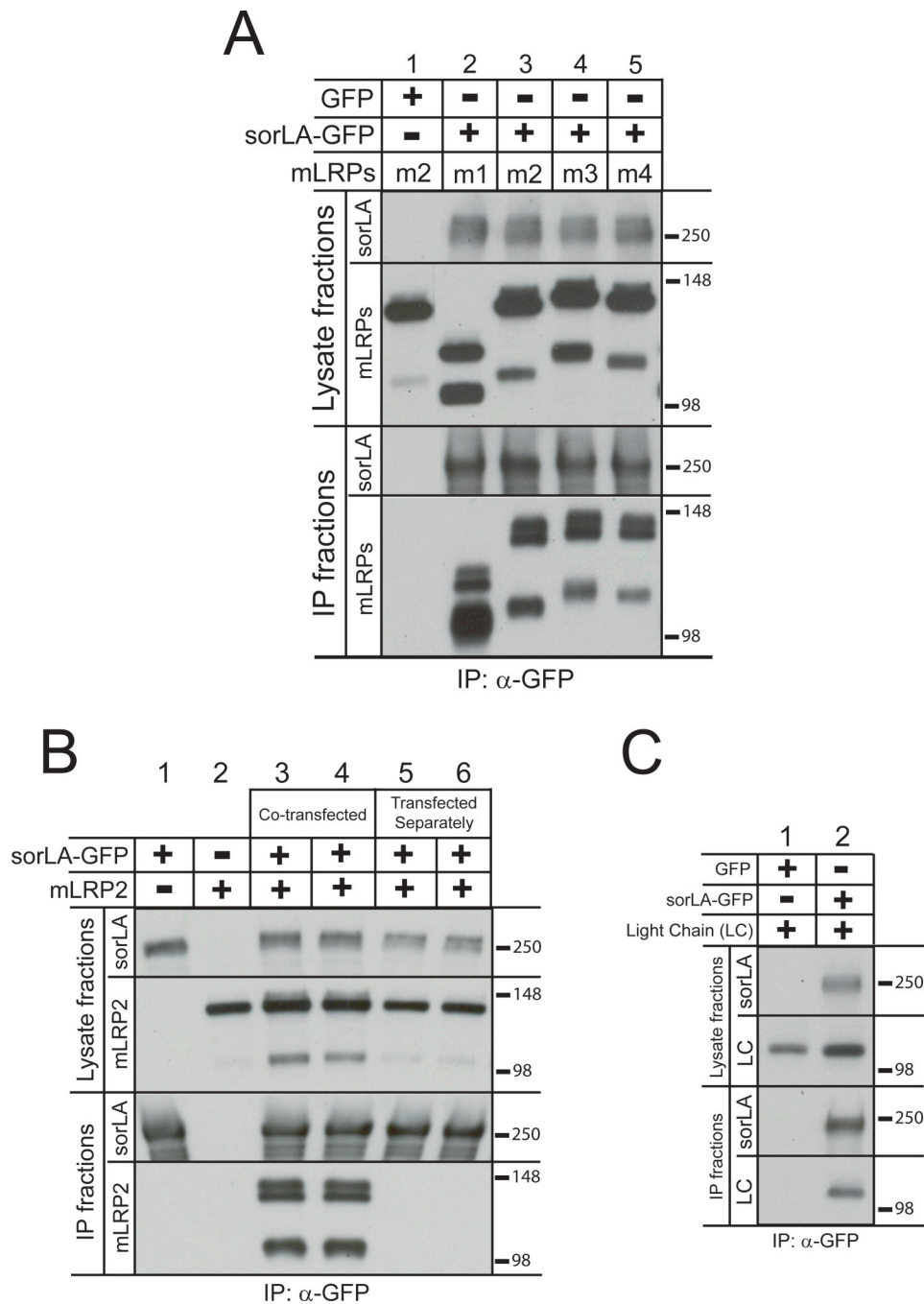


**Figure 2. LRP-sorLA interactions are mediated through the LRP light chain**

**A:** N2a cells were co-transfected with constructs encoding GFP or sorLA-GFP and myc-tagged mLRP1, 2, 3, or 4 (m1, m2, m3, m4). Forty-eight h after transfection, cell lysates were harvested and subjected to immunoprecipitation with anti-GFP antibody coupled to magnetic beads. Lysate and immunoprecipitation fractions were subjected to SDS-PAGE and Western analysis with anti-sorLA and anti-myc antibodies (n = 2). Two bands were detected for each mLRP receptor, corresponding to uncleaved (higher molecular weight bands) and furin-cleaved (lower molecular weight bands) receptors. In the case of mLRP1-myc, the lower band corresponds to the LRP light chain, as the myc tag is present at the C-terminus. Whereas for

myc-mLRP2, 3, and 4, the lower bands correspond to the respective truncated LRP heavy chains, as the myc tag is present at the N-terminus.

**B:** Constructs encoding sorLA-GFP and myc-mLRP2 were either co-transfected into cultures of N2a cells (lanes 3 and 4) or transfected separately into different cultures. Forty-eight h after transfection, the cells were harvested for immunoprecipitation. Immediately following cell lysis, lysates from the cultures transfected with either sorLA-GFP or myc-mLRP2 were combined (lanes 5 and 6) before proceeding with immunoprecipitation as in (B) (n = 4).

**C:** N2a cells were co-transfected with constructs encoding GFP or sorLA-GFP and myc-light chain (myc-LC). Forty-eight h after transfection, lysates were harvested and subjected to immunoprecipitation as in (B). Lysate and immunoprecipitation fractions were subjected to SDS-PAGE and Western blot with anti-sorLA and anti-myc antibodies (n = 2).



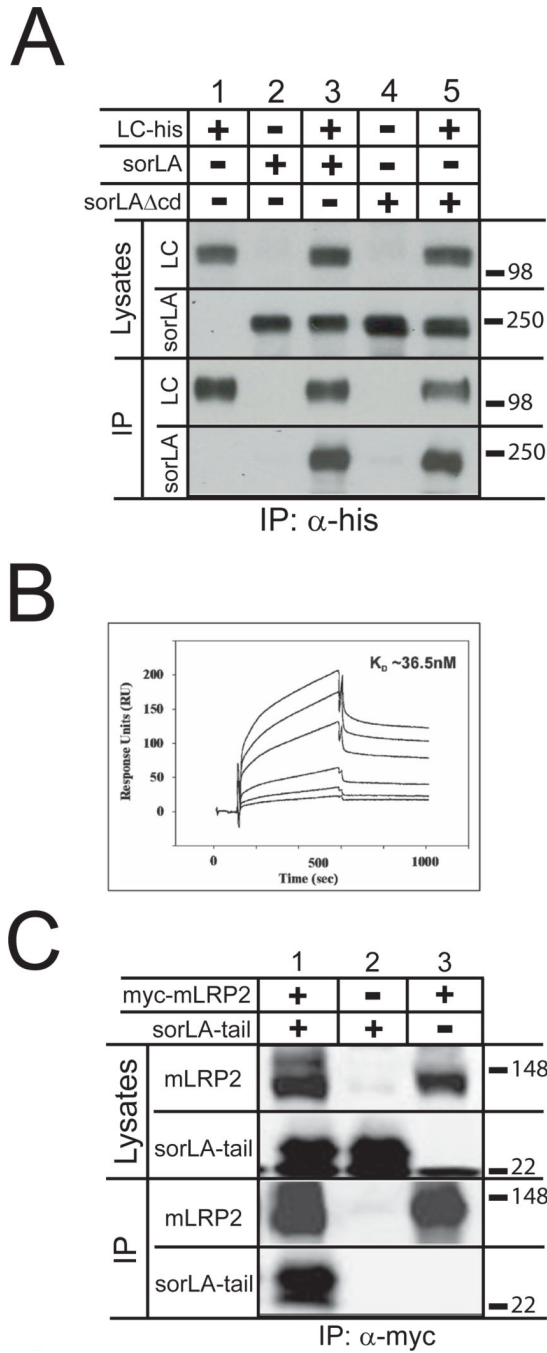


**Figure 3. LRP and sorLA exhibit luminal/extracellular domain and cytoplasmic domain interactions**

**A:** N2a cells were co-transfected with constructs encoding the LRP light chain with C-terminal myc and his tags (LC-his) and sorLA $\Delta$ cd, or with sorLA $\Delta$ cd alone. Twenty-four h after transfection, cells were harvested and lysates were subjected to immunoprecipitation using magnetic beads conjugated with anti-his antibody. Lysate and immunoprecipitation fractions were subjected to SDS-PAGE and Western blot with anti-sorLA and anti-myc antibodies (n = 2).

**B:** In surface plasmon resonance analysis, the sorLA ectodomain showed binding to immobilized LRP in concentrations of 0.05, 0.10, 0.20, 0.50, 1.0, and 2.0  $\mu\text{M}$ . The binding curves revealed a dissociation constant of  $K_D \sim 36.5 \text{ nM}$ .

**C:** N2a cells were co-transfected with constructs encoding the sorLA C-terminal tail (sorLA-tail) and myc-mLRP2. Twenty-four hours after transfection, cells were harvested and lysates were subjected to immunoprecipitation using magnetic beads conjugated with anti-myc antibody, followed by SDS-PAGE and Western analysis with anti-myc and anti-C-terminal sorLA antibodies ( $n = 2$ ).

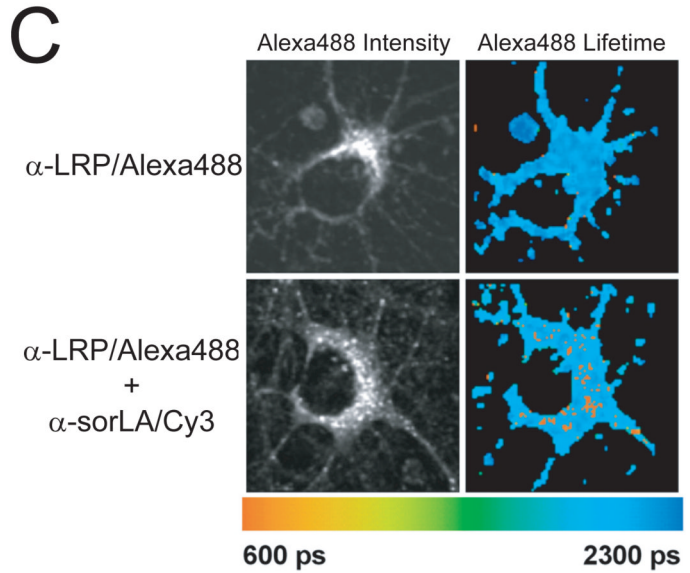
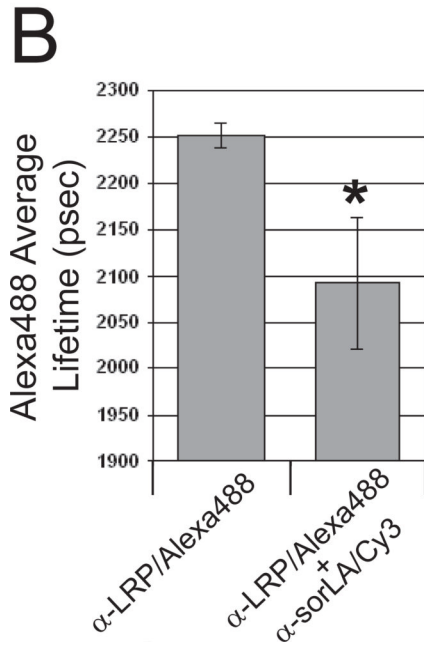
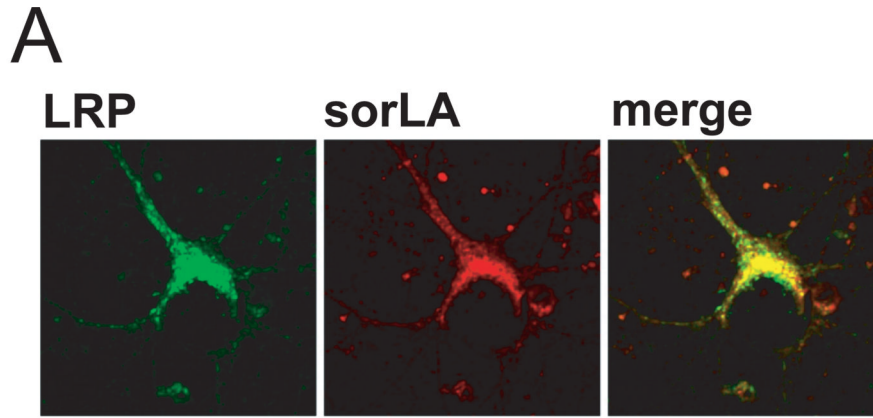


**Figure 4. LRP-sorLA interactions occur in perinuclear compartments of primary rat neurons**  
**A:** Rat primary neurons were immunostained for LRP with mouse anti-LRP 5A6 antibody, which was labelled with Alexa488 (left panel), and for sorLA with goat anti-sorLA antibody, which was labelled with Cy3 (middle panel). Overlay of these images showed co-localization mainly within perinuclear compartments (right panel).

**B:** Rat primary neurons were immunostained with mouse anti-LRP 5A6 antibody, labelled with Alexa488 (donor fluorophore), both without and with co-immunostaining with rabbit anti-N-terminal sorLA antibody labelled with Cy3 (acceptor fluorophore). The average lifetimes of the donor fluorophore are displayed in the bar graph (\*,  $p < 0.001$ ).

**C:** A representative image of the immunostained neurons from (B), in which the donor fluorescence intensity (left column) and lifetimes (right column) are shown. Fluorescence lifetimes are depicted as pseudocolored pixels with longer lifetimes towards the blue end of the spectrum and shorter lifetimes towards the orange end of the spectrum.